small methods
www.small-methods.com

Tailoring the Chemical Potential of Crystal Growth Units to Tune the Bulk Structure of Nanocrystals

Jiawei Zhang, Guifen Du, Huiqi Li, Qiaoli Chen, Qin Kuang, Zhiyuan Jiang, and Zhaoxiong Xie**

The intrinsic factors affecting the bulk structures of nanocrystallites are not well explored during crystallization. In this study, it is demonstrated that the chemical potential of growth units plays decisive role in governing the final structure of nanocrystals. It is found that the types of reaction vessels are able to vary the chemical potential of growth units, and make the Pt and Pd nanocrystals (NCs) unexpectedly evolve from the cyclic penta-twinned to the single-crystal nanostructures. In turn, it is concluded that the crystal growth units with lower chemical potential favor the formation of crystal nuclei with lower chemical potential during the nucleation. This new approach in tuning the bulk structures of NCs enriches the understanding of the crystallization process under supersaturated (nonequilibrium) condition, and would provide a general guidance for controlling nanocrystals with various thermodynamic forms.

Different from the molecular products that usually exist in a specific thermodynamically stable form, solid nanocrystals (NCs) have varied ultimate thermodynamic manifestations, for examples, NCs with various exposed facets, twinned nanostructures, and different crystal phases.[1–4] To date, no available universal theory can predict the final crystal forms of the as-obtained solid NCs through rational chemical synthesis, and current syntheses heavily rely on the inefficient trial-and-error processes.[5–7]

About a hundred years ago, the well-known Gibbs–Thomson equation ($\Delta\mu = 2\sigma v/r$) was proposed, by which the relationship between the crystallite size (r) and supersaturation ($\Delta\mu$) could be elucidated during crystal nucleation process.[8–10] In fact, the Gibbs–Thomson equation reflects the energy transformation between the solutes and newly formed solid crystal phase in the ideal condition of constant pressure and temperature.[9] In such crystallization system, the variation of Gibbs free energy of the can be express by Equation 1

$$dG = \mu_l dn_l + \mu_c dn_c + \sigma dS = 0 \quad (1)$$

where μ is the chemical potential, n is the number of moles of the corresponding species, S is the specific surface area of crystallites, σ is the specific surface energy of crystallites.

Accordingly, one may find that the excess energy should transform from solute with higher chemical potential ($\mu_l dn_l$) to the total surface energy of newly formed crystal phase (σdS), when the chemical potential of bulk crystal (μ_c) is a constant value. Hence, the higher supersaturation would result in smaller crystallites during nucleation process, in order to gain larger total surface energy.[8] Very recently, we found the Gibbs–Thomson equation is also applicable to the crystal growth process.[11] We then proposed a universal strategy for controlling the surface structure of NCs, that the high supersaturation of growth units can lead to the formation of crystal facet with high surface energy.[12]

Actually, the Gibbs–Thomson equation stand on the assumption that only one specific bulk crystal form is produced (μ_c is a constant value) during crystallization.[9] However, the presence of various final bulk structures for the NCs implies their chemical potentials of crystal nuclei may be dissimilar, especially in the nucleation stage.[2,3] As such, one question arises: whether the chemical potential of growth units could affect the chemical potential of newly formed crystal phase during nucleation process, and thus manipulating the bulk structure of solid NCs?

Herein, we demonstrate that the chemical potential of growth units is responsible for the transformation of bulk structure of solid NCs during crystallization. The shapes of Pt NCs evolve from cyclic penta-twinned (CPT) to single-crystalline (SC) nanostructures by simply switching the reaction vessels from Teflon to glass vial. We find the unexpected role of reaction vessels in tuning the chemical potential of growth units by elucidating the distinct nucleation behaviors in two different reaction vessels. And we propose that the chemical potential of growth units determine the final structure of NCs in the nonequilibrium nucleation process. This theory is further verified in controlled synthesis of CPT and SC Pd NCs, and is also used to explain the contradictory results and address unanswered questions

Dr. J. Zhang, G. Du, H. Li, Dr. Q. Chen, Prof. Q. Kuang, Prof. Z. Jiang, Prof. Z. Xie
State Key Laboratory of Physical Chemistry of Solid Surfaces
Collaborative Innovation Center of Chemistry for Energy Materials
College of Chemistry and Chemical Engineering
Xiamen University
Xiamen 361005, China
E-mail: qkuang@xmu.edu.cn; zxxie@xmu.edu.cn
Prof. Z. Xie
Pen-Tung Sah Institute of Micro-Nano Science and Technology
Xiamen University
Xiamen 361005, China
The ORCID identification number(s) for the author(s) of this article can be found under https://doi.org/10.1002/smtd.202000447.

DOI: 10.1002/smtd.202000447

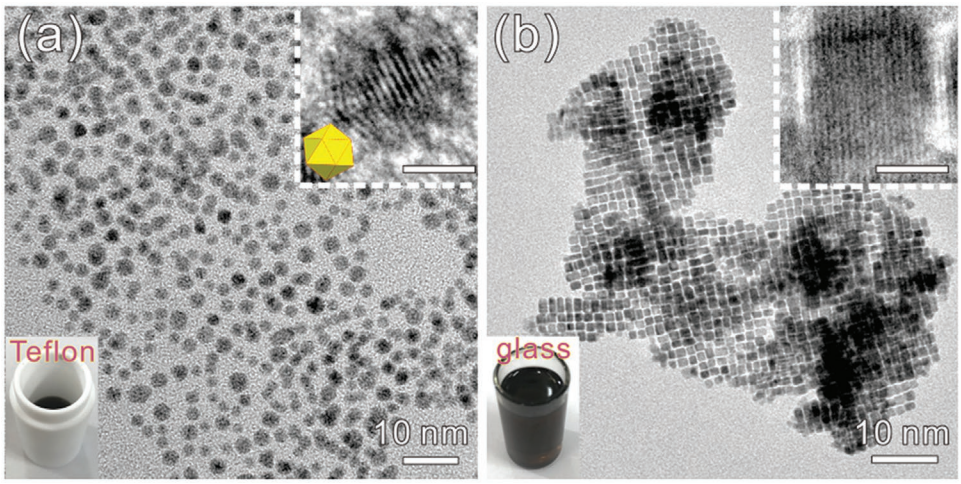

Figure 1. TEM and HRTEM images (inset) of Pt NCs synthesized in a) Teflon bottle and b) glass vial, while keeping all other experiment conditions the same. Scale bars in insets: 2 nm.

in previous studies.[13,14] This study would inspire the new approaches in the controlled synthesis of other thermodynamically metastable structures.

As shown in **Figure 1**a, the products obtained in the Teflon bottle were spherical, with particle sizes distributed in the range of 2.9 ± 1.2 nm. The high-resolution transmission electron microscope (HRTEM) analysis (inset in Figure 1a) further revealed these spherical nanoparticles were CPT icosahedra with twin boundaries (see Figure S1 for details in the Supporting Information). Interestingly, when the Teflon bottle was replaced with a glass vial while keeping all other experiment conditions unchanged, the obtained product consisted of 2.5 ± 0.8 nm SC cubic Pt NCs (Figure 1b). According to the energy-dispersive X-ray spectra and X-ray powder diffraction results, all the products are face-centered cubic Pt (Figures S2 and S3, Supporting Information). This shape transformation of Pt NCs caused by changing the reaction container was totally unexpected, and had not been reported before. This suggests that the crystallization behaviors of Pt NCs are different in these two containers.

CPT NCs can be considered as an assembly of five or twenty apex-sharing SC tetrahedra.[4,15–17] Thermodynamically, the formation of CPT nanostructures results from the competition between the increase of elastic strain energy caused by the lattice expansion in the twinned boundary region and the decreasing of surface free energy due to the small surface area. Therefore, the transformation between CPT and SC may occur by changing the surface free energy of NCs.[18,19] However, almost identical FTIR spectra indicated this "conservative" mechanism cannot explain the new observations in this study, where all the experimental conditions are the same except the reaction container (Figure S4, Supporting Information). Alternatively, crystal growth kinetics was considered to be the possible explanation as the low reduction rate favors the development of CPT NCs.[13] Nonetheless, the intrinsic role and driving force of reaction rate are still open questions.

It is known that Teflon and glass have distinct surface properties. The surface of Teflon bottle is hydrophobic and rough, while the glass vial possesses hydrophilic and smooth surface. Since the newly formed metal nuclei are hydrophobic, the hydrophobic and relatively rough surface of the Teflon bottle could provide abundant favorable nucleation sites. Therefore, the critical nucleation supersaturation in the Teflon bottle should be intrinsically lower than that in the glass vial, and crystal nucleation should appear earlier accordingly. To verify this hypothesis, the Tyndall effect was used to uncover the formation of Pt nuclei. When the reaction stopped at 0.5 h, a bright light beam was observed in the solution of Teflon-based synthesis (**Figure 2**). In contrast, no light beam was observed in the glass vial until the reaction time was extended to 1 h (Figure S5, Supporting Information). This confirmed that the crystal nucleation in the Teflon bottle was indeed earlier than that in the glass vial. In other words, the critical supersaturation (representing the thermodynamic driving force for crystallization) for nucleation in the Teflon bottle, was lower than that in the glass vial.[9]

As mentioned above, Gibbs–Thomson equation considers only one specific crystal phase is produced (constant μ_c).[8,9] Therefore, one can tune the μ_l directly to influence the size or the surface energy of target NCs (Equation 1).[12] However, in present study, the bulk structures are different, which means they have different μ_c. Besides, the previous understanding

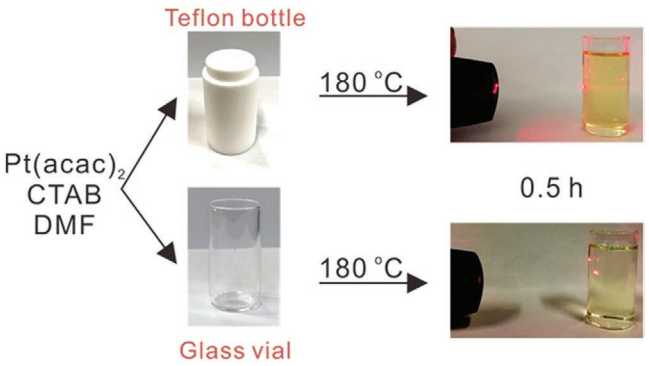

Figure 2. The synthesis pathways and photographs of the suspension of Pt NCs synthesized in different reaction containers.

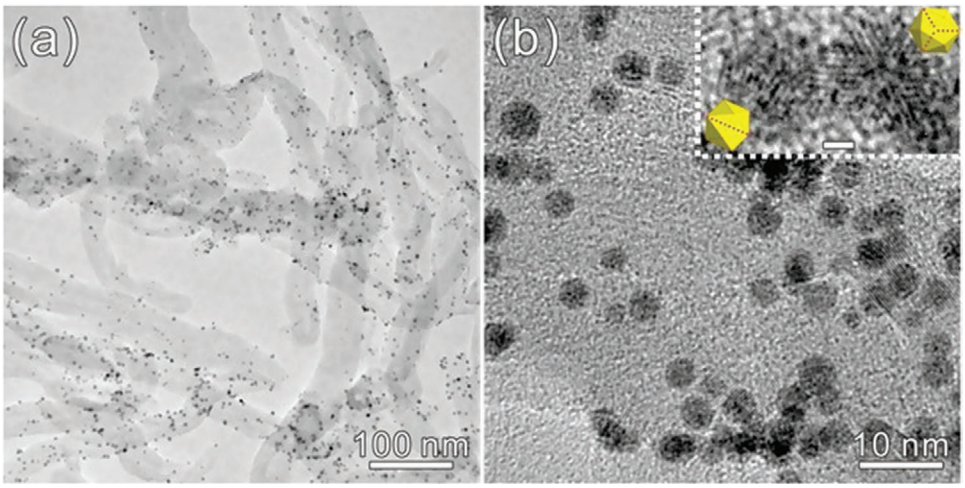

Figure 3. a) Low- and b) high-magnification TEM images of CPT icosahedral Pt supported on CNTs. Scale bar in the inset: 1 nm.

about the crystal growth mechanism (e.g., Gibbs–Curie–Wulff role) is largely drawn from the assumption that the crystal grows under near-saturated (near-equilibrium) condition.[9] Nevertheless, the formation of CPT NCs is determined in the nucleation stage, where highly supersaturated (nonequilibrium) condition is involved.[20] As such, it is not suitable to explain the formation of CPT NCs under nonequilibrium conditions with the theory of near-equilibrium growth, and a new mechanism should be proposed.

Through looking into the Equation 1 again, it can reasonably infer that the variation of μ_l could also govern the μ_c. During the nucleation process, lower μ_l would favor the crystalline with lower μ_c, i.e., lower critical supersaturated condition is conducive to the formation of nuclei with lower chemical potential. Given that CPT NCs were the main product in the Teflon bottle, it can be concluded that CPT nuclei form under relatively low supersaturation (lower μ_l) conditions, because the formation of CPT NCs stems from the CPT nuclei.[4,6,20]

In order to further demonstrate the role of chemical potential in tailoring the bulk structures, more experiments were conducted. For instance, in a glass vial, we can intentionally reduce the critical nucleation supersaturation (i.e., the chemical potential of crystal growth unit) by introducing additional nucleation sites, such as carbon nanotubes (CNTs). **Figure 3** shows highly dispersed icosahedral NCs on the CNTs were prepared in glass vial, instead of face-to-face assembled SC Pt nanocubes. Besides, the chemical potential of growth units is positively correlated to the reduction rate of precursors.[12] Therefore, the chemical potential of growth units in Teflon bottle can be increased by adding reductants. As expected, when 15 mg ascorbic acid (AA) was added, the product was assembled SC Pt nanocubes rather than dispersed CPT Pt icosahedra (Figure S6, Supporting Information). Alternatively, the reduction rate can be finely tuned by the amount of hexadecyltrimethylammonium bromide (CTAB), as bromide ions can adjust the effective concentration and reduction potential of noble metal ions by forming complexes.[6,21] The reduction rate would be faster when fewer CTAB is used. By reducing the amount of CTAB from 30 to 0 mg, the proportion of SC Pt nanocubes in the product gradually increased (Figure S7, Supporting Information). Based on the above results, it is easy to understand previous confused experimental results, why CPT NCs can still be formed when using capping agents that can strongly adsorb and decrease the surface energy of NCs (Thermodynamically, SC NCs should form).[14] It is the reduced reduction rate of metal ions when involving capping agents. The lower the reduction rate is, the lower the chemical potential of growth units is, which is in turn conducive to the formation of CPT nuclei. Clearly, the underlying role of tuning the apparent reaction rate is regulating the chemical potentials of growth units, which in turn affects the final bulk structures.[13]

Importantly, the concept of chemical potential-dependent nanostructure evolution can also be used to control the structures of Pd NCs (Figure S8, Supporting Information). When the Pd NCs were prepared in the Teflon bottle, the products were icosahedral NCs (**Figure 4**a). According to the HRTEM analyses, the crystal lattice spacing was 0.23 nm, belonging to the (111) plane of Pd (Figure 4b). At the same time, CPT nature with multi-boundaries was clearly observed. The fast Fourier transform (FFT) images of individual icosahedron along the two- and threefold axes further demonstrate the successful synthesis of CPT NCs.[14,22,23] Obviously, the low chemical potential in the Teflon bottle gave the formation of CPT Pd icosahedra. Alternatively, when the Pd NCs were produced in the glass vial, which endowed the growth units with high chemical potential, octahedral Pd NCs accompanied by lots of small SC nanoparticles were produced (Figure 4c; Figure S9, Supporting Information). The SC nature was confirmed by the HRTEM image with continues lattice fringes, and typical SC FFT pattern. Again, when AA was added in the Teflon bottle to elevating the chemical potential of growth units, the products transformed from CPT Pd icosahedra to small SC truncated octahedral nanoparticles (Figure 4d; Figure S10, Supporting Information).

All the above results demonstrated that high chemical potential of growth environment could result in high supersaturation of growth units, thus producing crystallites with high chemical potential (SC nuclei and SC NCs in this case). This conclusion can be easily understood in the synthesis of NCs with different surface energies.[12] However, in this study, the low-potential system would lead to the final CPT nanostructure,

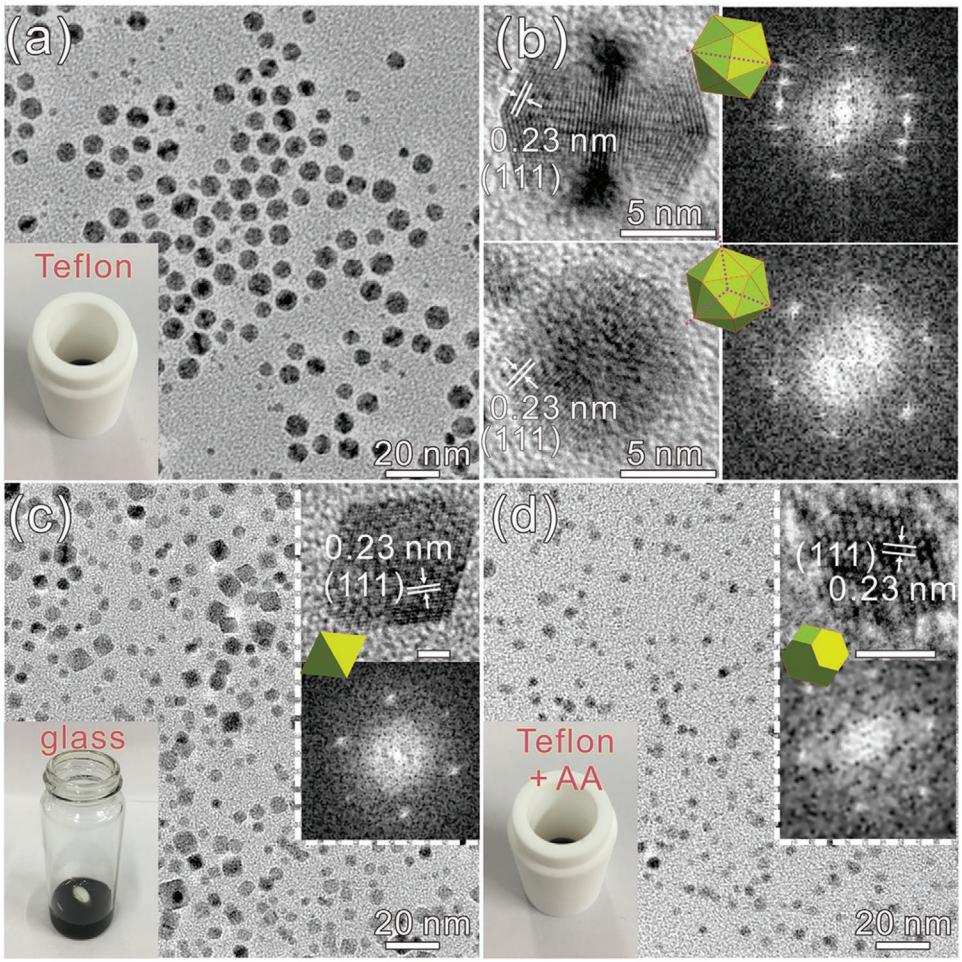

Figure 4. a) TEM image of CPT icosahedral Pd NCs synthesized in the Teflon bottle. b) HRTEM images of an icosahedral Pd NC oriented along twofold axis (top), and threefold axis (bottom) projections and corresponding FFT images and geometrical models. c) TEM image of SC octahedral Pd NCs synthesized in the glass vial. d) TEM image of SC Pd NCs synthesized in the Teflon bottle with additional 30 mg AA. The insets in (c) and (d) are the HRTEM images of a single Pd NC with corresponding FFT image along [110] direction. Scale bars in insets: 2 nm.

which at first glances should possess a high chemical potential because of its additional elastic strain energy.[4,16,17] This confusion can be elucidated by the fact that, the CPT nuclei usually prevail over SC nuclei because of their lower total energy during the nucleation stage of crystal growth.[24] As such, low-chemical-potential growth units facilitate the formation of CPT nucleus with low chemical potential, finally forming the CPT nanostructures.

In conclusion, this work provided a fundamental understanding of the role of chemical potential in turning final nanostructures. Briefly, when the critical supersaturation of crystal nucleation is low, the CPT nuclei (with low chemical potential) prevail over SC nuclei at the nucleation stage, finally forming the CPT nanostructures. In other words, during the nucleation, the crystal growth units with lower chemical potential favor the formation of crystal nuclei with lower chemical potential. This study not only expands our understanding about the complex crystallization process under nonequilibrium conditions (supersaturated condition), but also would open a new avenue to direct the controlled synthesis of solid inorganic NCs with various thermodynamic forms

Experimental Section

Chemicals: Platinum acetylacetonate ($Pt(acac)_2$), sodium tetrachloropalladate (II) (Na_2PdCl_4) were purchased from Kunming Noble Metal Institute. *N*, *N*-dimethylformamide (DMF) and L-ascorbic acid (AA) were purchased from Sinopharm Chemical Reagent Co. Ltd (Shanghai, China). Poly(vinyl-pyrrolidone) (PVP, $M_W \approx 55\,000$) was acquired from Sigma-Aldrich. CTAB (>99%) was bought from J&K. Ethylene glycol (EG) was obtained from J. T. Baker. Carbon nanotubes with 90% purity and typical lengths of 5–15 µm were acquired from Shenzhen Nanotech Port Co. Ltd (Shenzhen China). The water used in all experiments was ultrapure (>18.0 MΩ cm). All reagents were used as received without further purification.

Synthesis of CPT Pt Icosahedra and SC Pt Nanocubes: To synthesize CPT Pt icosahedra, $Pt(acac)_2$ (4 mg) and CTAB (30 mg) were dissolved in 10 mL of DMF in a 20 mL of Teflon-lined stainless-steel autoclave. The steel was kept in 180 °C for 15 h before it was cooled to room temperature. The black product was collected by centrifugation and washed with ethanol three times and water for once. To synthesize SC Pt nanocubes, $Pt(acac)_2$ and CTAB were dissolved in 10 mL of DMF in a glass vessel and then transferred to 20 mL Teflon-lined stainless-steel autoclave, while keeping all other things the same.

Synthesis of CPT Pd Icosahedra and SC Pd NCs: To synthesize CPT Pd icosahedra, PVP (30 mg) was dissolved in 2 mL of EG in a 20 mL

of Teflon bottle and was placed in oil bath at 150 °C under magnetic stirring. At the same time, Na_2PdCl_4 (1.6 mg) was dissolved in 1 mL of EG and heated at 60 °C. After about 5 min, 1 mL of EG containing Na_2PdCl_4 was rapidly injected into the Teflon bottle mentioned above, using a pipette. After reaction for about 3 h, the Teflon bottle was cooled in water. The product was collected by centrifugation and washed with acetone and water for two times each. When AA (30 mg) was additionally added in the Teflon bottle, or the Teflon bottle was replaced by a 20 mL glass vessel while keeping other experiment parameters unchanged, the products were SC Pd nanoparticles or Pd octahedral NCs, respectively.

Characterization of Samples: The morphology and structure of as-prepared Pt or Pd NCs were investigated by transmission electron microscopy (TEM, JEOL JEM 2100) with an accelerating voltage of 200 kV. All TEM samples were prepared by depositing a few drops of sample suspension fully ultrasonicated in ethanol on a copper grid coated with carbon film.

Supporting Information

Supporting Information is available from the Wiley Online Library or from the author.

Acknowledgements

This work was supported by the National Key Research and Development Program of China (2017YFA0206500 and 2017YFA0206801), the National Natural Science Foundation of China (Nos. 21931009, 21721001, 21773190, and 21671163).

Conflict of Interest

The authors declare no conflict of interest.

Keywords

chemical potential, crystal growth, noble metal, supersaturation, twin

Received: June 11, 2020
Revised: July 27, 2020
Published online: September 1, 2020

[1] Y. Chen, Z. Lai, X. Zhang, Z. Fan, Q. He, C. Tan, H. Zhang, *Nat. Rev. Chem.* **2020**, *4*, 243.
[2] H. Li, X. Wang, *Acc. Chem. Res.* **2019**, *52*, 780.
[3] J. Lai, W. Niu, R. Luque, G. Xu, *Nano Today* **2015**, *10*, 240.
[4] S. Zhou, M. Zhao, T. Yang, Y. Xia, *Mater. Today* **2019**, *22*, 108.
[5] Y. Xia, X. Xia, H. Peng, *J. Am. Chem. Soc.* **2015**, *137*, 7947.
[6] M. L. Personick, C. A. Mirkin, *J. Am. Chem. Soc.* **2013**, *135*, 18238.
[7] Y. Wang, J. He, C. Liu, W. H. Chong, H. Chen, *Angew. Chem., Int. Ed.* **2015**, *54*, 2022.
[8] P. Wynblatt, N. A. Gjostein, *Acta Metall.* **1976**, *24*, 1165.
[9] I. V. Markov, *Crystal Growth for Beginners: Fundamentals of Nucleation, Crystal Growth and Epitaxy*, 2nd ed., World Scientific, Singapore **2003**.
[10] N. T. Thanh, N. Maclean, S. Mahiddine, *Chem. Rev.* **2014**, *114*, 7610.
[11] H. X. Lin, Z. Lei, Z. Jiang, C. Hou, D. Liu, M. Xu, Z. Tian, Z. Xie, *J. Am. Chem. Soc.* **2013**, *135*, 9311.
[12] J. Zhang, H. Li, Q. Kuang, Z. Xie, *Acc. Chem. Res.* **2018**, *51*, 2880.
[13] Y. Wang, H. C. Peng, J. Liu, C. Z. Huang, Y. Xia, *Nano Lett.* **2015**, *15*, 1445.
[14] G. Du, J. Zhang, Q. Chen, Q. Kuang, Z. Xie, *Chem. Commun.* **2018**, *54*, 10855.
[15] M. Song, G. Zhou, N. Lu, J. Lee, E. Nakouzi, H. Wang, D. Li, *Science* **2020**, *367*, 40.
[16] H. Huang, H. Jia, Z. Liu, P. Gao, J. Zhao, Z. Luo, J. Yang, J. Zeng, *Angew. Chem., Int. Ed.* **2017**, *56*, 3594.
[17] J. Wu, L. Qi, H. You, A. Gross, J. Li, H. Yang, *J. Am. Chem. Soc.* **2012**, *134*, 11880.
[18] Z. Niu, Q. Peng, M. Gong, H. Rong, Y. Li, *Angew. Chem., Int. Ed.* **2011**, *50*, 6315.
[19] S. Bao, J. Zhang, Z. Jiang, X. Zhou, Z. Xie, *J. Phys. Chem. Lett.* **2013**, *4*, 3440.
[20] L. M. Liz-Marzan, M. Grzelczak, *Science* **2017**, *356*, 1120.
[21] Y. Xiong, H. Cai, B. J. Wiley, J. Wang, M. J. Kim, Y. Xia, *J. Am. Chem. Soc.* **2007**, *129*, 3665.
[22] Y. Yang, J. Zhang, Y. Wei, Q. Chen, Z. Cao, H. Li, J. Chen, J. Shi, Z. Xie, L. Zheng, *Nano Res.* **2018**, *11*, 656.
[23] W. Zhu, A. X. Yin, Y. W. Zhang, C. H. Yan, *Chem. - Eur. J.* **2012**, *18*, 12222.
[24] F. Baletto, C. Mottet, R. Ferrando, *Phys. Rev. B* **2001**, *63*, 155408.